A Miniaturized Monolithic 2.4/5.7 GHz Concurrent Dual-Band Low Noise Amplifier Using InGaP/GaAs HBT Technology

KUN-NAN LIAO and YO-SHENG LIN, *Member, IEEE*
Department of Electrical Engineering
National Chi-Nan University
University Rd. Puli, Nantou Hsien, Taiwan
REPUBLIC OF CHINA

Abstract: - This paper presents the design and experimental results of a miniaturized monolithic 2.4/5.7 GHz concurrent dual-band low noise amplifier with cascade configuration using InGaP/GaAs HBT technology for the first time. The first stage of the LNA provides high gain and input matching simultaneously at both 2.4 GHz and 5.7 GHz bands. The output matching of the second stage is realized by shunt-shunt feedback. It consumes only 9 mW power and achieves transducer gains (S_{21}) of 24.8 dB and 15.7 dB, input return losses (S_{11}) of -23.6 dB and -22.6 dB, output return losses (S_{22}) of -15.3 dB and -21.5 dB, reverse isolation (S_{12}) of -48.0 dB and -44.4 dB, and noise figures of 3.42 dB and 2.72 dB at 2.4 GHz and 5.7 GHz, respectively. The LNA only occupies an area of 650 μm × 300 μm excluding the test pads because only two inductors are used.

Key-Words: - Low Noise Amplifier, Dual-band, Concurrent, InGaP/GaAs HBT.

1 Introduction

Wireless communication has evolved into a world of multi-standards/multi-services with operating frequencies of 900 MHz/1.8 GHz/1.9 GHz bands for GSM, 1.5 GHz band for GPS and 2.4 GHz/5.2 GHz/5.7 GHz bands for WLAN. Therefore, it is desirable to combine two or more standards in one mobile unit [1]-[2]. The primary challenge in designing multi-band transceivers is increasing the functionality of such communication systems while minimizing the number of additional hardware such as low noise amplifiers (LNAs). Typical design strategies have used different LNAs for different frequency bands [2]-[5]. However, this method inevitably increases the cost and power dissipation. Recently, a 2.45/5.25 GHz concurrent dual-band CMOS LNA with excellent performances has been reported [5]. However, in this circuit, off-chip capacitors and inductors are used. In addition, a 2.4/5.2/5.7 GHz triple bands SiGe HBT LNA achieved by switching between different base bias currents (I_B) is reported [6]. The disadvantage of this circuit is its small IIP_3. To realize low cost and low power consumption and to operate at 2.4/5.7 GHz bands simultaneously, a single LNA suitable for 2.4/5.7 GHz dual-band operation is needed. Therefore, in this paper, for the first time, we present the design and implementation of a 2.4/5.7 GHz concurrent dual-band LNA using InGaP/GaAs HBT technology.

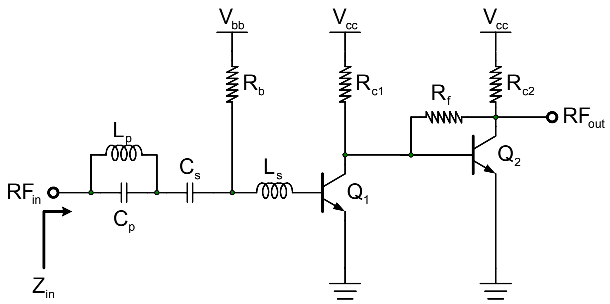

Fig. 1 The complete circuit of the 2.4/5.7 GHz concurrent dual-band InGaP/GaAs HBT LNA.

2 Circuit Design

To realize high transducer gain and good reverse isolation, a cascade configuration was adopted for the 2.4/5.7 GHz concurrent dual-band InGaP/GaAs HBT LNA. The complete circuit of the LNA was shown in Fig. 1. The approach introduced in Ref. [5] was adopted to achieve the input impedance matching and noise matching of the LNA. The wideband output matching of the LNA was realized by using a shunt-shunt feedback architecture, which had the advantages of stabilizing gain and minimizing chip area (because no LC component was used in the output terminal).

2.1 Input Impedance and Noise Matching

In the first stage, the size and bias of the transistor were chosen appropriately to minimize power consumption and to obtain low noise figure by keeping the device current density close to the minimum noise figure region. Besides, the input impedance matching was achieved at the two bands of interest. This can be explained by the small signal equivalent circuit model seen at the input port as shown in Fig. 2. The input impedance is given by:

$$Z_{in} \approx \left(R_p' // sL_p // \frac{1}{sC_p} \right) + \left[\frac{1}{s(C_S + C_\pi + C_M)} + sL_s + (R_N + r_b + R_s) \right]$$
$$= Z_p + Z_s \quad (1)$$

where $Z_p = R_p' // sL_p // \frac{1}{sC_p}$ is a shunt RLC network, $Z_s = \frac{1}{s(C_S + C_\pi + C_M)} + sL_s + (R_N + r_b + R_s)$ is a series RLC network. The real parts of Z_{in} (50Ω) at the 2.4/5.7 GHz bands mainly come from Z_p. The uninterested frequency (notch frequency f_{notch}) was set as 3.5 GHz. At the notch frequency, the input impedance is a maximum because of the bad input impedance matching (that is, large reflection coefficient). The imaginary part of Z_p is inductive and capacitive for frequencies lower and higher than f_{notch}, respectively, while the imaginary part of Z_s is capacitive and inductive for frequencies lower and higher than f_{notch}, respectively. By appropriately selecting the values of L_p, C_p, C_s, and L_s, the imaginary parts of Z_p and Z_s are canceled at both 2.4 GHz and 5.7 GHz, and the summation of the real part of Z_p and Z_s approach 50Ω at both 2.4 and 5.7 GHz. Since the minimization of the noise figure of the LNA is very important, the matching network was designed to achieve the minimum oval noise figure, but still to maintain a reasonable input impedance matching at both of the frequencies of interest. In this circuit, the sum of the impedance of Z_p and Z_s were reduced to its minimum in order to minimize the noise figure [5].

2.2 Output Matching

The output matching of the second stage was realized by a common shunt-shunt feedback technique [7]. This technique would stabilize gain but cause the degradation of noise figure because of the feedback resistors. This disadvantage was not critical in the second stage as its contribution to overall noise figure was reduced by the power gain of the first stage.

In order to minimize chip area, the fewer inductors, the better. Therefore, resistors were used as output loadings in place of LC resonant circuit. Another advantage of using resistive loads was wideband matching. That is why this LNA was capable of offering high gain at both 2.4 GHz and 5.7 GHz. Furthermore, the input and output matching were pretty good.

3 Experimential Results

An InGaP/GaAs HBT IC process with f_t=40 GHz was used to fabricate the LNA. The die photograph of the finished monolithic 2.4/5.7 GHz dual-band LNA is shown in Fig. 3. The layout was done in a uni-directional fashion to avoid signal coupling between the input and output. The RF input and output terminals were placed on opposite sides of the chip to improve port-to-port isolation. The total chip area was only 650 μm × 300 μm excluding the test pads. This LNA drained 5 mA current at supply voltage of 1.8 V; that is to say, it only consumed 9 mW power.

The noise and scattering parameters were measured on wafer using an automated NP5 measurement system from ATN Microwave Inc. This LNA achieved transducer gains (S_{21}) of 24.8 dB and 15.7 dB, and input return losses (S_{11}) of -23.6 dB and -22.6 dB at 2.4 GHz and 5.7 GHz frequency bands, respectively, as shown in Fig. 4 and 5. As can be seen in Fig. 6, the measured reverse isolation (S_{12}) for the LNA was quite good, i.e. -48.0 dB and -44.4 dB, at 2.4 GHz and 5.7 GHz frequency bands, respectively, and with less than -40 dB of isolation for frequencies lower than 7 GHz. The measured noise figure (NF) was 3.42 dB and 2.72 dB at 2.4 GHz and 5.7 GHz frequency bands, respectively, as shown in Fig. 8. Finally, two-tone-intermodulation measurement was performed and results are shown in Fig. 9. Clearly, an $IIP_3 = -17$ dBm was obtained.

The performances at 5.7 GHz of our 2.4/5.7 GHz concurrent dual-band InGaP/GaAs LNA (NF of 2.72 dB, and S_{21} of 15.7 dB) were better than those (NF of 4.5 dB, and S_{21} of 15.5 dB) of the 2.45/5.25 GHz concurrent dual-band CMOS LNA at 5.25 GHz with a bonding wire as the gate inductor using 0.35 μm CMOS technology [5]. This means the performance of our InGaP/GaAs dual-band LNA can be much better than that of its CMOS version without the use of bonding wire.

4 Conclusion

A low power monolithic concurrent 2.4/5.7 GHz dual-band LNA using InGaP/GaAs HBT technology is presented for the first time. The total chip area is only 650 μm × 300 μm excluding the test pads. S_{21} of 24.8 dB and 15.7 dB, S_{11} of -23.6 dB and -22.6 dB, S_{12} of -48.0 dB and -44.4 dB, and NF of

3.42 dB and 2.72 dB are achieved at 2.4/5.7 GHz bands, respectively. The total power consumption is only 9 mW at +1.8 V power supply. Compared to the recently published GaAs and SiGe HBT LNA results (see Table 1), the performance of this work is pretty good and occupies the smallest chip area.

5 Acknowledgement

The authors are grateful for the measurement support from High Frequency Measurement Center of the NDL.

References:

[1] T. Antes and C. Conkling, RF chip set fits multimode cellular/PCS handsets, *Microwave RF*, Dec. 1996, pp. 177-186.

[2] S. Wu and B. Razavi, A 900-MHz/1.8-GHz CMOS receiver for dual-band applications, *IEEE J. Solid-State Circuits*, vol.33, no.12, Dec. 1998, pp. 2178-2185.

[3] R. Magoon, I. Koullias, L. Steigerwald, W. Domino, N. Vakillian, E. Ngompe, M. Damgaard, K. Lewis, A. Molnar, A triple-band 900/1800/1900 MHz low-power image-reject front-end for GSM, *ISSCC Dig. of Tech. Papers,* Feb. 2001, pp. 408-409.

[4] K. L. Fong, Dual-band high-linearity variable-gain low-noise amplifiers for wireless applications, *ISSCC Dig. of Tech. Papers,* Feb. 1999, pp.224-225.

[5] H. Hashemi and A. Hajimiri, Concurrent dual-band CMOS low noise amplifiers and receiver architectures, *Symp. on VLSI Circ. Dig.,* Jun. 2001, pp.247-250.

[6] P. W. Lee, H. W. Chiu, T. L. Hsieh, G. W. Huang, and S. S. Lu, A SiGe Low Noise Amplifier for 2.4/5.2/5.7 GHz WLAN Applications, *IEEE International Solid-State Circuits Conference*, 2003.

[7] C. D. Hull R. G. Meyer, Principles of wideband feedback amplifier design, *INT. J. High speed Electron.*, vol.3, no.1, Mar. 1992, pp. 53-93.

[8] K. W. Kobayashi, et al., Ultra- Low DC Power GaAs HBT S- and C-Band Low Noise Amplifiers for portable Wireless Applications, *IEEE Trans. MTT*, no.12, Dec. 1995, pp. 3055-3061.

[9] M. Soyuer, J-O. Plouchart, H. Ainspan, and J. Burghartz, A 5.8 GHz 1-V low noise amplifier in SiGe bipolar technology, *IEEE Radio Frequency Integrated Circuits Symposium*, 1997, pp.19-22.

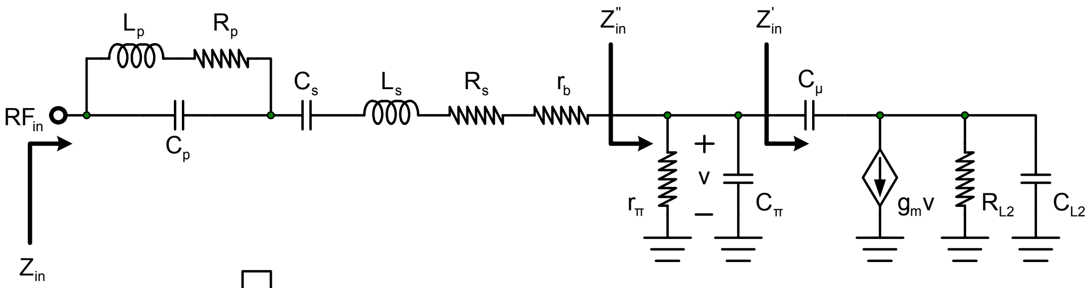

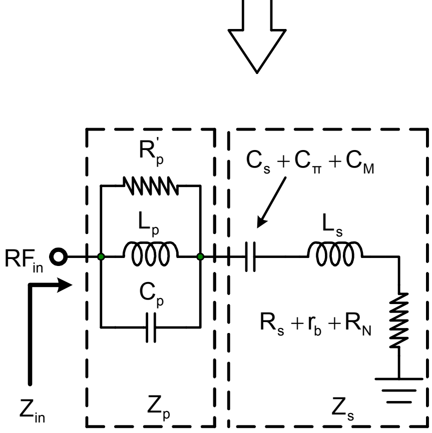

$$Z_{in}^{'} \approx \frac{1}{sC_{\mu}(1+g_m R_{L2})} + \left[\frac{R_{L2}}{1+g_m R_{L2}} + \frac{g_m R_{L2}^2 C_{L2}}{(1+g_m R_{L2})^2 C_{\mu}}\right] = \frac{1}{sC_M} + R_M$$

$$Z_{in}^{''} \approx \frac{1}{s(C_{\pi}+C_M)} + \frac{1}{\omega^2 (C_{\pi}+C_M)^2 (r_{\pi}+R_M)} = \frac{1}{sC_N} + R_N$$

$$Z_{in} \approx \left(R_p^{'} // sL_p // \frac{1}{sC_p}\right) + \left[\frac{1}{s(C_s+C_{\pi}+C_M)} + sL_s + (R_s+r_b+R_N)\right] = Z_p + Z_s$$

Fig. 2 The small signal equivalent model seen at the input terminal of the 2.4/5.7 GHz concurrent dual-band GaInP/GaAs HBT LNA.

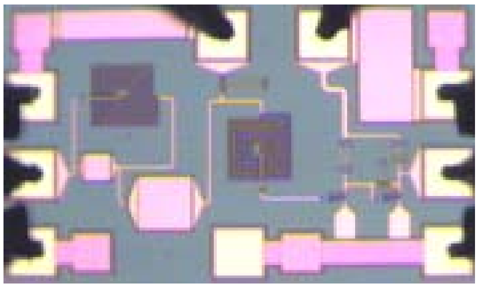

Fig. 3 The die photograph of the2.4/5.7 GHz concurrent dual-band GaInP/GaAs HBT LNA.

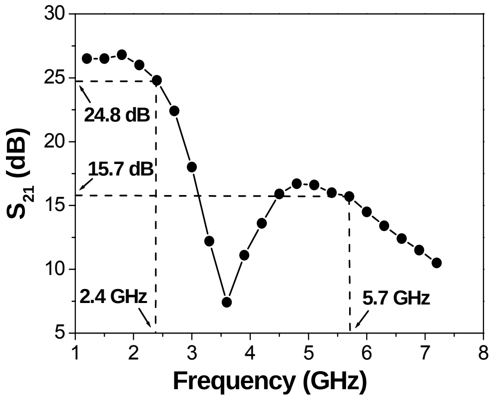

Fig. 4 The measured transducer gains (S_{21}) of the 2.4/5.2 GHz dual-band LNA.

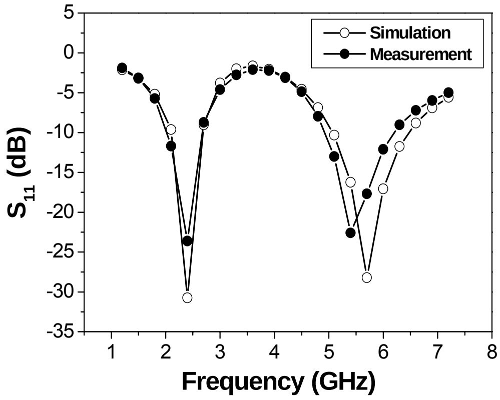

Fig. 5 The simulated and measured input return loss (S_{11}) of the 2.4/5.2 GHz dual-band LNA.

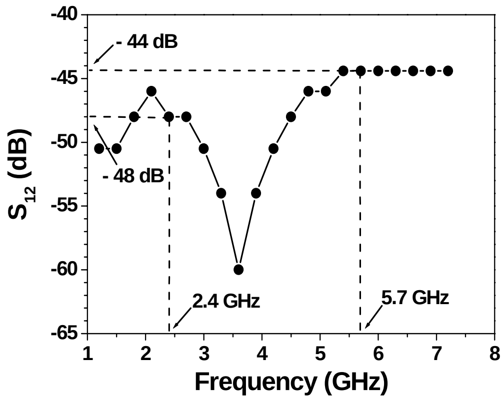

Fig. 6 The measured reverse isolation (S_{12}) of the 2.4/5.2 GHz dual-band LNA.

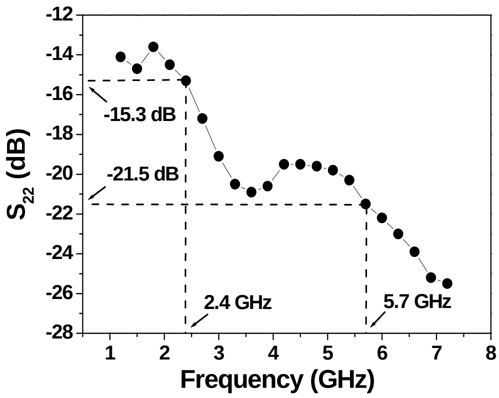

Fig. 7 The measured output return loss (S_{22}) of the 2.4/5.2 GHz dual-band LNA.

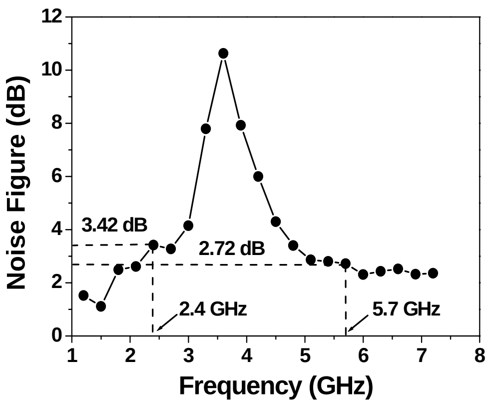

Fig. 8 The measured noise figure (NF) of the 2.4/5.2 GHz dual-band LNA.

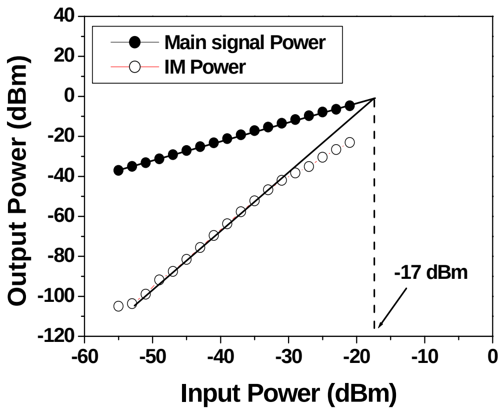

Fig. 9 The measured third order inter-modulation characteristics of the 2.4/5.2 GHz dual- band LNA.

Table 1 Comparison of the performance of this work and the recently published GaAs and SiGe HBT LNA results.

Technology	Center frequency (GHz)	S21 (dB)	S11 (dB)	NF (dB)	Power (mW)	Area (mm^2)
GaAs HBT [8]	5	16.2	-6	2.4	72	1.59x0.83
SiGe HBT [9]	5.8	13	-6	2.1**	13	0.7x0.8
CMOS [5]	2.45	14*	-25	2.3**	10	0.8x0.8
CMOS [5]	5.25	15.5*	-15	4.5**	10	0.8x0.8
This work	2.4	24.8	-23.6	3.42	9	0.65x0.3
This work	5.7	15.7	-22.6	2.72	9	0.65x0.3

* Voltage gain   ** Off-chip